

## Indications for Lifshitz transitions in the nodal-line semimetal ZrSiTe induced by interlayer interaction

M. Krottenmüller,<sup>1,\*</sup> M. Vöst,<sup>2,\*</sup> N. Unglert<sup>1,†</sup>,<sup>2,\*</sup> J. Ebad-Allah,<sup>1,3</sup> G. Eickerling<sup>1,2</sup>,<sup>3</sup> D. Volkmer<sup>1,4</sup>,<sup>5</sup> J. Hu,<sup>5</sup> Y. L. Zhu<sup>1,6,7</sup>,<sup>8</sup>  
Z. Q. Mao,<sup>6,7</sup> W. Scherer,<sup>2,†</sup> and C. A. Kuntscher<sup>1,‡</sup>

<sup>1</sup>Experimentalphysik II, Institute of Physics, University Augsburg, 86159 Augsburg, Germany

<sup>2</sup>Chair of Chemical Physics and Materials Science, Institute of Physics, University of Augsburg, 86159 Augsburg, Germany

<sup>3</sup>Department of Physics, Tanta University, 31527 Tanta, Egypt

<sup>4</sup>Chair of Solid State and Materials Chemistry, Institute of Physics, University of Augsburg, 86159 Augsburg, Germany

<sup>5</sup>Department of Physics, University of Arkansas, Fayetteville, Arkansas 72701, USA

<sup>6</sup>Department of Physics, Pennsylvania State University, University Park, Pennsylvania 16803, USA

<sup>7</sup>Department of Physics and Engineering Physics, Tulane University, New Orleans, Louisiana 70118, USA



(Received 11 December 2019; accepted 29 January 2020; published 19 February 2020)

The layered material ZrSiTe is currently extensively investigated as a nodal-line semimetal with Dirac-like band crossings protected by nonsymmorphic symmetry close to the Fermi energy. A recent infrared spectroscopy study on ZrSiTe under external pressure found anomalies in the optical response, providing hints for pressure-induced phase transitions at  $\approx 4.1$  and  $\approx 6.5$  GPa. By pressure-dependent Raman spectroscopy and x-ray diffraction measurements combined with electronic band structure calculations we find indications for two pressure-induced Lifshitz transitions with major changes in the Fermi surface topology in the absence of lattice symmetry changes. These electronic phase transitions can be attributed to the enhanced interlayer interaction induced by external pressure. Our findings demonstrate the crucial role of the interlayer distance for the electronic properties of layered van der Waals topological materials.

DOI: [10.1103/PhysRevB.101.081108](https://doi.org/10.1103/PhysRevB.101.081108)

Topological materials such as topological insulators [1], Dirac [2], Weyl [3–5], or line-node semimetals [6,7] are of great fundamental interest due to their exotic nature of electronic phases, and thus heavily investigated nowadays. They usually exhibit extraordinary material properties, for example, high carrier mobility and unusual magnetoresistance [8–10]. Topological nontrivial phases often occur in layered materials with weak interlayer bonding, where the single layers behave rather as isolated two-dimensional (2D) objects, enabling the exfoliation to atomically thin 2D crystals with numerous possible applications [11–15]. Since the forces between the layers of such structures are usually weak, they are highly compressible perpendicular to the layers, and a dimensional crossover from 2D to 3D can be induced by external pressure. Generally, layered materials are prone to pressure-induced phenomena, and electronic topological transitions [16] are expected to be induced [17–19] and were suggested to occur in layered BiTeBr [20], BiTeI [21,22], 1T-TiTe<sub>2</sub> [23], and the group V selenides and tellurides Bi<sub>2</sub>Se<sub>3</sub>, Bi<sub>2</sub>Te<sub>3</sub>, and Sb<sub>2</sub>Te<sub>3</sub> [24–27].

“Electronic transitions” in metals were first introduced by Lifshitz in 1960 as transitions where the topology of the Fermi surface (FS) changes as a result of the continuous deformation

under high external pressure [16]. Examples for pressure-induced alterations of the FS topology are the conversion of an open Fermi surface, such as a corrugated cylinder-type Fermi surface typical for layered materials, to a closed one, or the appearance of a new split-off region of the FS. Importantly, the changes in the Fermi surface topology during such a so-called Lifshitz transition are not related to a change in the lattice symmetry [16].

In this work we find indications for two Lifshitz transitions in the layered van der Waals material ZrSiTe under external pressure, resulting from the enhanced interlayer interaction. ZrSiTe belongs to the family of compounds ZrXY ( $X = \text{Si}, \text{Ge}, \text{Sn}$  and  $Y = \text{O}, \text{S}, \text{Se}, \text{Te}$ ), which are nodal-line semimetals [28,29]. The materials ZrXY exhibit largely varying interlayer bonding [11,30], with ZrSiTe being a clear outlier towards more 2D character [28,29]. According to recent infrared reflectivity measurements under external pressure [31], ZrSiTe is highly sensitive to pressure. In particular, several optical parameters showed anomalies in their pressure dependence at the critical pressures  $P_{c1} \approx 4.1$  GPa and  $P_{c2} \approx 6.5$  GPa, suggesting the occurrence of two phase transitions of either electronic or structural type. For the clarification of the pressure-induced effects in ZrSiTe, we carried out Raman spectroscopy and x-ray diffraction measurements under external pressure and density-functional-theory (DFT) electronic band structure calculations.

ZrXY compounds, with  $X$  being a carbon group atom and  $Y$  a chalcogen atom, have a PbFCl-type tetragonal structure with space group  $P4/nmm$  and lattice parameters  $a = 3.70 \text{ \AA}$

\*These authors contributed equally to this work.

†wolfgang.scherer@physik.uni-augsburg.de

‡christine.kuntscher@physik.uni-augsburg.de

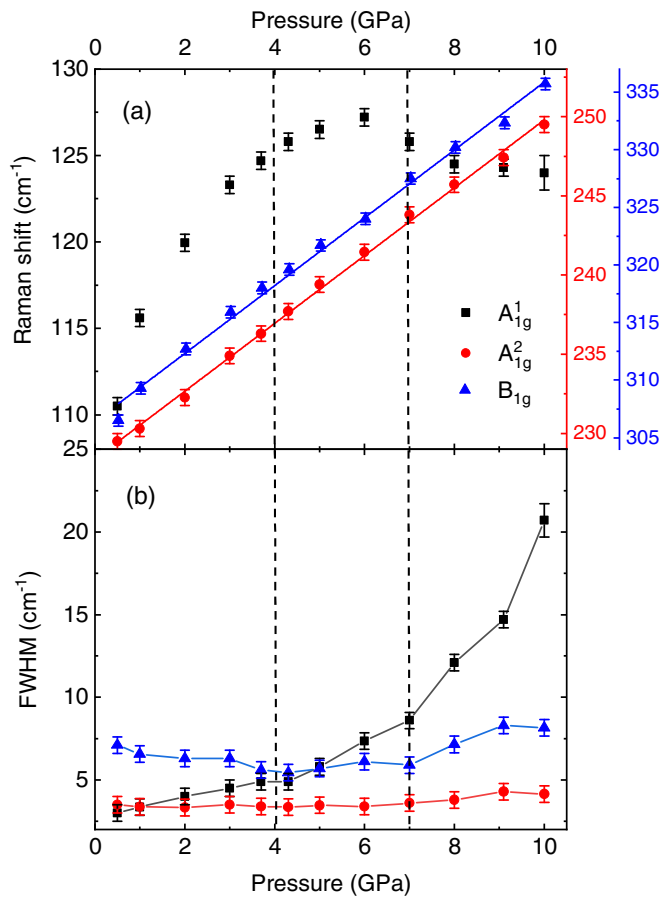


FIG. 1. (a) Frequencies of the *basal-plane* Raman modes  $A_{1g}^1$ ,  $A_{1g}^2$ , and  $B_{1g}$  in ZrSiTe as a function of pressure. The red and blue lines are linear fits of the pressure evolution of the  $A_{1g}^2$  and  $B_{1g}$  mode frequencies, respectively. (b) FWHM of the Raman modes  $A_{1g}^1$ ,  $A_{1g}^2$ , and  $B_{1g}$  in ZrSiTe as a function of pressure. The two vertical dashed lines indicate the two critical pressures  $\sim 4$  and  $\sim 7$  GPa.

and  $c = 9.51 \text{ \AA}$  for ZrSiTe (see Fig. S1 in the Supplemental Material [32]) [28,29]. The layered crystal structure of Zr $XY$  is built from quintuple layers of [Y-Zr-X-Zr-Y] parallel to the  $ab$  plane. Due to the layered nature, the occurrence of so-called rigid-layer phonon modes is expected [33], where atomic layers move against each other along the  $c$  direction. The *basal-plane* Raman spectra of ZrSiY ( $Y = \text{S, Se, Te}$ ) and ZrGeY ( $Y = \text{S, Se}$ ) single crystals consist of three modes [see Fig. S1(b) in the Supplemental Material [32]] which can be assigned to the  $A_{1g}^1$ ,  $A_{1g}^2$ , and  $B_{1g}$  modes. The atomic displacements of these three Raman modes consist of mostly out-of-plane motions along the  $c$  direction [34–36]. Hereby, the modes  $A_{1g}^1$  and  $A_{1g}^2$  can be assigned to motions of Zr and Y atoms and the mode  $B_{1g}$  to motions of X atoms.

According to the pressure-dependent Raman spectra of ZrSiTe (see Fig. S2 in the Supplemental Material [32]) all three phonon modes  $A_{1g}^1$ ,  $A_{1g}^2$ , and  $B_{1g}$  harden with increasing pressure up to 6 GPa and are observed up to the highest measured pressure (10 GPa). Importantly, there are no signs for pressure-induced structural phase transitions. The pressure dependence of the frequencies was extracted by Lorentz fitting and is depicted in Fig. 1(a). The pressure dependence of the

modes  $A_{1g}^2$  and  $B_{1g}$  is linear with the pressure coefficients 2.1 and  $2.9 \text{ cm}^{-1}/\text{GPa}$ , respectively. In contrast, we observe a pronounced nonlinearity of the pressure-induced shift of the  $A_{1g}^1$  mode: Up to  $\sim 4$  GPa this mode shows a strong hardening with increasing pressure, which saturates between 4 and 6 GPa. Remarkably, above  $\sim 7$  GPa the  $A_{1g}^1$  mode softens with increasing pressure. Also the pressure behavior of the full-width at half-maximum (FWHM) of the  $A_{1g}^1$  mode is distinct [see Fig. 1(b)]: Whereas the FWHM of the  $A_{1g}^2$  and  $B_{1g}$  modes shows no clear pressure dependence, the FWHM of  $A_{1g}^1$  increases linearly up to  $\sim 7$  GPa, with an anomaly at  $\sim 4$  GPa above which the linear pressure coefficient increases. Above  $\sim 7$  GPa the FWHM of  $A_{1g}^1$  increases strongly [38].

In analogy to ZrSiS and PbFCl, the  $A_{1g}^1$  mode is ascribed to the relative motion between two weakly bonded Zr-Y units [35,36]. Due to the in-phase motion of the Y layer and the adjacent Zr layer [see Fig. S1(a) in the Supplemental Material [32] for illustration] it can be considered as a rigid-layer mode, which is very sensitive to changes in interlayer interactions induced, e.g., by external pressure. In particular, the frequencies of rigid-layer modes can be employed to monitor the changes in the interlayer bonding, as demonstrated for layered chalcogenide crystals [33]. Accordingly, the observed strong pressure-induced hardening of the rigid-layer  $A_{1g}^1$  mode up to 6 GPa signals a strong enhancement of the interlayer interaction in ZrSiTe during pressure application. It is interesting to note that, previously, pressure-induced anomalies in the frequency and FWHM of Raman modes were interpreted in terms of electronic phase transitions (EPTs) in several cases [22,23,25–27,39]. In particular, the FWHM can be strongly affected by changes in the electron-phonon coupling, which can serve as an indirect signature for an EPT [23].

The pressure-induced changes in the crystal structure of ZrSiTe were investigated by single-crystal x-ray diffraction measurements. The pressure dependence of the lattice parameters  $a$  and  $c$  and of the unit cell volume  $V$  is depicted in Fig. 2. The volume  $V$  decreases monotonically with increasing pressure  $P$  and can be described by a second-order Murnaghan equation of state (EOS) [40]:

$$V(P) = V_0[(B'_0/B_0)P + 1]^{-1/B'_0}, \quad (1)$$

where  $B_0$  is the bulk modulus,  $B'_0$  its pressure derivative, and  $V_0$  the volume, all at  $P = 0$  GPa. The so-obtained bulk modulus amounts to  $B_0 = 40.9 \pm 2.5$  GPa and its derivative to  $B'_0 = 9.2 \pm 1.0$ . The value of  $B'_0$  of ZrSiTe is enhanced compared to the value  $B'_0 = 4$  typical for 3D materials with isotropic elastic properties, which signals the layered character of ZrSiTe. For comparison, the corresponding values of  $B_0$  and  $B'_0$  of graphite amount to 33.8 GPa and 8.9, respectively, [41] and for the more 3D sister compound ZrSiS  $141 \pm 4.5$  GPa and  $5.1 \pm 0.5$ , respectively [35].

The lattice parameters  $a$  and  $c$  show a distinct pressure dependence for the pressure range below and above  $\sim 7$  GPa (see Fig. 2). Whereas parameter  $a$  is hardly affected by pressure (please note the scale), parameter  $c$  monotonically decreases up to 7 GPa and is pressure independent above 7 GPa. Obviously, the  $c$  direction perpendicular to the layers shows the highest compressibility and is most affected at low pressures. This finding is also illustrated by the  $c/a$

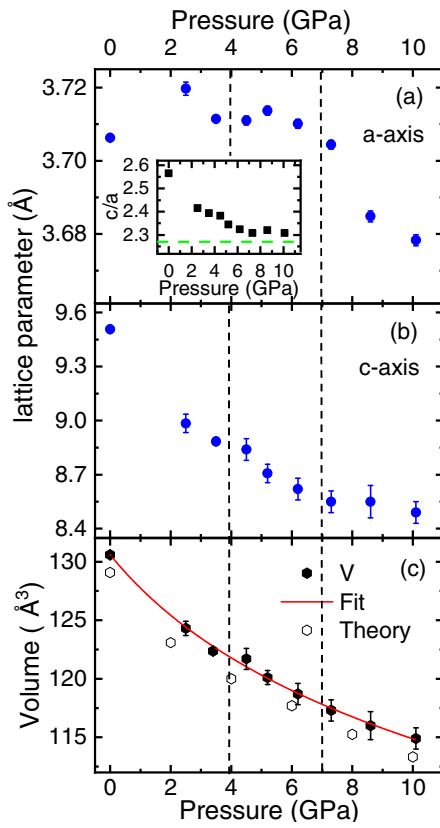


FIG. 2. (a),(b) Pressure dependence of the lattice parameters  $a$  and  $c$  of ZrSiTe. Inset: Pressure dependence of the  $c/a$  ratio. The horizontal dashed line marks the  $c/a$  ratio of ZrSiS at ambient pressure [35,37]. (c) Volume  $V$  of the unit cell as a function of pressure together with the calculated values. The solid line is a fit of the experimental data with a second-order Murnaghan EOS as defined in the text. The two vertical dashed lines indicate the two critical pressures  $\sim 4$  and  $\sim 7$  GPa.

ratio, which basically follows the pressure dependence of the parameter  $c$  [see inset of Fig. 2(a)]. It is important to note that, despite these changes, we can exclude the occurrence of a crystal symmetry change for pressures up to 10 GPa (see Supplemental Material [32] for details).

For an interpretation of the experimental results, we performed first-principles DFT electronic structure calculations. The electronic band structure of ZrSiTe for selected pressures together with the corresponding FS is shown in Figs. 3(a)–3(c) and 3(e)–3(g), respectively. In agreement with earlier reports [30,42,43], the ambient-pressure electronic band structure of ZrSiTe contains a nodal line, which is gapped due to spin-orbit coupling. Additional Dirac-like band crossings, which are protected by nonsymmorphic symmetry against gapping (called nonsymmorphic Dirac crossings in the following) appear close to the Fermi energy  $E_F$  at the  $X$  and  $R$  points of the Brillouin zone (BZ). The nodal line close to  $E_F$ , which is found in all Zr $XY$  compounds, is formed by Si  $sp_x p_y$ -Zrd hybrid orbitals [29,30]. In fact, the two linearly crossing (touching) bands in Zr $XY$  are located along a surface in the BZ, forming an effective nodal plane [30]. The FS of ZrSiTe has a diamond-rod shape with additional four, rather flat pillars and four electron pockets [see Fig. 3(e)].

From our pressure-dependent calculations it is obvious that the electronic band structure of ZrSiTe is highly sensitive to external pressure. With increasing pressure, the diamond-shaped FS shrinks to be small, and the pillars are disrupted as well. Overall, the FS is drastically reduced up to  $\sim 4$  GPa (see Fig. 3 and the Supplemental Material [32]), in agreement with the reported decrease of the plasma frequency [31]. Above 4 GPa this trend is reversed, i.e., the FS enlarges with increasing pressure, and above  $\sim 8$  GPa some parts of the FS are connected, forming corrugated cylinders with side arms and a diamond-shaped component. This is in full agreement with the behavior of the plasma frequency, showing an increase above 4 GPa followed by a plateau-like saturation above  $\sim 7$  GPa, reaching a value close to the ambient-pressure one [31]. From these drastic pressure-induced changes of the FS, we infer that ZrSiTe undergoes two Lifshitz transitions in the pressure range 0–10 GPa.

The pressure-dependent energy positions of the Dirac crossings in the electronic band structure of ZrSiTe and ZrSiS are depicted in Figs. 3(i)–3(k). With increasing pressure the Dirac crossings forming the nodal line are shifted towards  $E_F$  and even cross  $E_F$  above  $\sim 4$  GPa. The nonsymmorphic Dirac crossings are strongly pushed away from the Fermi level. At the highest studied pressure (10 GPa) the electronic band structure and FS of ZrSiTe have strong similarities with the sister compound ZrSiS at ambient pressure [see Figs. 3(d) and 3(h)], with the nonsymmorphic Dirac crossings at energies  $\pm 0.75$  eV away from  $E_F$  [Fig. 3(j)]. Hence, high-pressure ZrSiTe provides the opportunity to extract the properties of the nodal-line state without the influence of the nonsymmorphic Dirac state, similar to ZrSiS but with larger spin-orbit coupling. Together with the fact that the  $c/a$  ratio of ZrSiTe at 10 GPa is close to that of ambient-pressure ZrSiS [35,37] [see Fig. 2(a)], these findings further stress the importance of the interlayer interaction for the electronic properties of the Zr $XY$  compound family.

According to our results, we propose the following scenario for ZrSiTe under pressure: For  $0 \lesssim P \lesssim 4$  GPa a pressure-induced dimensional crossover from layered to more 3D is induced within the parent tetragonal phase, as indicated by the drastic decrease in the  $c/a$  ratio and the strong hardening of the  $A_{1g}^1$  mode, concomitant with its intensity increase. At  $\sim 4$  GPa a Lifshitz transition occurs with drastic changes in the electronic band structure and a shrinkage of the FS, leading to an intermediate phase for pressures  $4 \lesssim P \lesssim 7$  GPa. At  $\sim 7$  GPa another Lifshitz transition with an enlargement of the FS occurs, and the electronic band structure of ZrSiTe becomes similar to that of ambient-pressure ZrSiS.

Recently, a temperature-induced Lifshitz transition was observed in the layered topological material ZrTe<sub>5</sub> [44,45]. It was speculated that this transition is induced by the variation of the interlayer interaction with temperature. Our results for the van der Waals material ZrSiTe show that layered topological materials are prone to Lifshitz transitions driven by the pressure-induced enhancement of the interlayer interaction.

In summary, by Raman spectroscopy we observed anomalies in the pressure dependence of the frequency and linewidth of the rigid-layer phonon mode in ZrSiTe, in the absence of any lattice symmetry change according to pressure-dependent x-ray diffraction results. The pressure behavior of the Raman

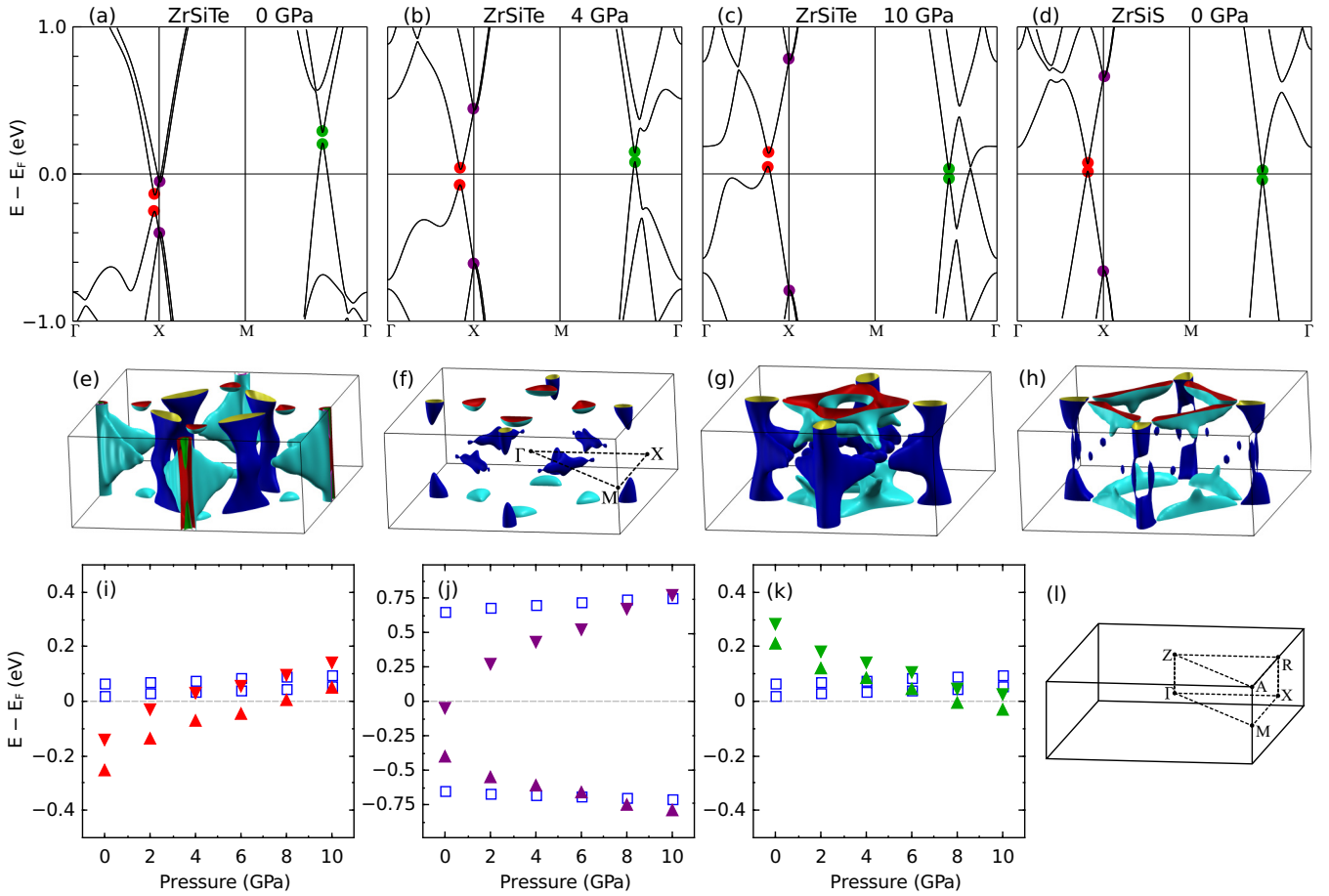


FIG. 3. (a)–(c) Electronic band structure of ZrSiTe at selected pressures, with the Dirac crossings marked by colored points. (d) Electronic band structure of ZrSiS at ambient pressure. (e)–(g) Fermi surface of ZrSiTe at selected pressures. (h) Fermi surface of ZrSiS at ambient pressure. (i)–(k) Energy position of Dirac crossings in the electronic band structure of ZrSiTe [triangles, color coding according to the points in (a)–(c)] and ZrSiS (squares) as a function of pressure. (l) High-symmetry points in the tetragonal BZ.

mode can be explained by the drastic decrease of the  $c/a$  lattice parameter ratio concomitant with an enhanced interlayer interaction. DFT band structure calculations indicate the occurrence of two Lifshitz transitions at  $\sim 4$  GPa and  $\sim 7$  GPa with drastic changes in the Fermi surface topology. The Lifshitz transitions can be attributed to the pressure-induced enhancement of the interlayer interaction. Our results demonstrate the crucial role of the interlayer distance in determining the electronic structure of the layered, nodal-line

semimetal ZrSiTe, and we propose that this finding holds for layered van der Waals topological materials in general.

We thank Hana Bunzen for technical support. C.A.K. acknowledges financial support from the Deutsche Forschungsgemeinschaft (DFG), Germany, through Grant No. KU 1432/13-1. The sample synthesis and characterization efforts were supported by the US Department of Energy under Grant No. DE-SC0019068.

- 
- [1] L. Fu, C. L. Kane, and E. J. Mele, *Phys. Rev. Lett.* **98**, 106803 (2007).
- [2] S. M. Young, S. Zaheer, J. C. Y. Teo, C. L. Kane, E. J. Mele, and A. M. Rappe, *Phys. Rev. Lett.* **108**, 140405 (2012).
- [3] X. Wan, A. M. Turner, A. Vishwanath, and S. Y. Savrasov, *Phys. Rev. B* **83**, 205101 (2011).
- [4] A. A. Soluyanov, D. Gresch, Z. Wang, Q. S. Wu, M. Troyer, X. Dai, and B. A. Bernevig, *Nature (London)* **527**, 495 (2015).
- [5] N. P. Armitage, E. J. Mele, and A. Vishwanath, *Rev. Mod. Phys.* **90**, 015001 (2018).
- [6] A. A. Burkov, M. D. Hook, and L. Balents, *Phys. Rev. B* **84**, 235126 (2011).
- [7] C. Fang, Y. Chen, H.-Y. Kee, and L. Fu, *Phys. Rev. B* **92**, 081201(R) (2015).
- [8] M. Neupane, S.-Y. Xu, R. Sankar, N. Alidoust, G. Bian, C. Liu, I. Belopolski, T.-R. Chang, H.-T. Jeng, H. Lin, A. Bansil, F. Chou, and M. Z. Hasan, *Nat. Commun.* **5**, 3786 (2014).
- [9] Y.-Y. Lv, B.-B. Zhang, X. Li, S.-H. Yao, Y. B. Chen, J. Zhou, S.-T. Zhang, M.-H. Lu, and Y.-F. Chen, *Appl. Phys. Lett.* **108**, 244101 (2016).

- [10] R. Sankar, G. Peramaiyan, I. P. Muthuselvam, C. J. Butler, K. Dimitri, M. Neupane, G. N. Rao, M.-T. Lin, and F. C. Chou, *Sci. Rep.* **7**, 40603 (2017).
- [11] Q. Xu, Z. Song, S. Nie, H. Weng, Z. Fang, and X. Dai, *Phys. Rev. B* **92**, 205310 (2015).
- [12] L. M. Schoop, M. N. Ali, C. Strasser, A. Topp, A. Varykhalov, D. Marchenko, V. Duppel, S. S. P. Parkin, B. V. Lotsch, and C. R. Ast, *Nat. Commun.* **7**, 11696 (2016).
- [13] K. Deng, G. Wan, P. Deng, K. Zhang, S. Ding, E. Wang, M. Yan, H. Huang, H. Zhang, Z. Xu, J. Denlinger, A. Fedorov, H. Yang, W. Duan, H. Yao, Y. Wu, S. Fan, H. Zhang, X. Chen, and S. Zhou, *Nat. Phys.* **12**, 1105 (2016).
- [14] M. Zhang, X. Wang, F. Song, and R. Zhang, *Adv. Quantum Technol.* **2**, 1800039 (2019).
- [15] J. Ma, L. Zheng, S. Wu, Z. Liu, S. Zhou, and D. Sun, *2D Mater.* **6**, 32001 (2019).
- [16] I. M. Lifshitz, *JETP* **11**, 1130 (1960).
- [17] Z. Zhu, Y. Cheng, and U. Schwingenschlögl, *Phys. Rev. Lett.* **108**, 266805 (2012).
- [18] M. Yang, Y. Z. Luo, M. G. Zeng, L. Shen, Y. H. Lu, J. Zhou, S. J. Wang, I. K. Sou, and Y. P. Feng, *Phys. Chem. Chem. Phys.* **19**, 29372 (2017).
- [19] D. Bassanezi, E. O. Wrasse, and T. M. Schmidt, *Mater. Res. Express* **5**, 015051 (2018).
- [20] A. Ohmura, Y. Higuchi, T. Ochiai, M. Kanou, F. Ishikawa, S. Nakano, A. Nakayama, Y. Yamada, and T. Sasagawa, *Phys. Rev. B* **95**, 125203 (2017).
- [21] X. Xi, C. Ma, Z. Liu, Z. Chen, W. Ku, H. Berger, C. Martin, D. B. Tanner, and G. L. Carr, *Phys. Rev. Lett.* **111**, 155701 (2013).
- [22] Yu. S. Ponosov, T. V. Kuznetsova, O. E. Tereshchenko, K. A. Kokh, and E. V. Chulkov, *JETP Lett.* **98**, 557 (2013).
- [23] V. Rajaji, U. Dutta, P. C. Sreeparvathy, S. Ch. Sarma, Y. A. Sorb, B. Joseph, S. Sahoo, S. C. Peter, V. Kanchana, and C. Narayana, *Phys. Rev. B* **97**, 085107 (2018).
- [24] A. Polian, M. Gauthier, S. M. Souza, D. M. Trichêes, J. Cardoso de Lima, and T. A. Grandi, *Phys. Rev. B* **83**, 113106 (2011).
- [25] O. Gomis, R. Vilaplana, F. J. Manjón, P. Rodríguez-Hernández, E. Pérez-González, A. Muñoz, V. Kucek, and C. Drasar, *Phys. Rev. B* **84**, 174305 (2011).
- [26] R. Vilaplana, D. Santamaría-Pérez, O. Gomis, F. J. Manjón, J. González, A. Segura, A. Muñoz, P. Rodríguez-Hernández, E. Pérez-González, V. Marín-Borrás, V. Muñoz-Sanjosé, C. Drasar, and V. Kucek, *Phys. Rev. B* **84**, 184110 (2011).
- [27] R. Vilaplana, O. Gomis, F. J. Manjón, A. Segura, E. Pérez-González, P. Rodríguez-Hernández, A. Muñoz, J. González, V. Marín-Borrás, V. Muñoz-Sanjosé, C. Drasar, and V. Kucek, *Phys. Rev. B* **84**, 104112 (2011).
- [28] C. Wang and T. Hughbanks, *Inorg. Chem.* **34**, 5524 (1995).
- [29] W. Bensch, O. Helmer, M. Muhler, H. Ebert, and M. Knecht, *J. Phys. Chem.* **99**, 3326 (1995).
- [30] J. Ebad-Allah, J. F. Afonso, M. Krottenmüller, J. Hu, Y. L. Zhu, Z. Q. Mao, J. Kunes, and C. A. Kuntscher, *Phys. Rev. B* **99**, 125154 (2019).
- [31] J. Ebad-Allah, M. Krottenmüller, J. Hu, Y. L. Zhu, Z. Q. Mao, and C. A. Kuntscher, *Phys. Rev. B* **99**, 245133 (2019).
- [32] See Supplemental Material at <http://link.aps.org/supplemental/10.1103/PhysRevB.101.081108> for details about sample preparation, Raman measurements, XRD measurements, calculations, and additional experimental and theoretical results, which includes Refs. [46–72].
- [33] R. Zallen and M. Slade, *Phys. Rev. B* **9**, 1627 (1974).
- [34] W. Zhou, H. Gao, J. Zhang, R. Fang, H. Song, T. Hu, A. Stroppa, L. Li, X. Wang, S. Ruan, and W. Ren, *Phys. Rev. B* **96**, 064103 (2017).
- [35] R. Singha, S. Samanta, S. Chatterjee, A. Pariari, D. Majumdar, B. Satpati, L. Wang, A. Singha, and P. Mandal, *Phys. Rev. B* **97**, 094112 (2018).
- [36] Y. A. Sorb, N. Subramanian, and T. R. Ravindran, *J. Phys.: Condens. Matter* **25**, 155401 (2013).
- [37] C. C. Gu, J. Hu, X. L. Chen, Z. P. Guo, B. T. Fu, Y. H. Zhou, C. An, Y. Zhou, R. R. Zhang, C. Y. Xi, Q. Y. Gu, C. Park, H. Y. Shu, W. G. Yang, L. Pi, Y. H. Zhang, Y. G. Yao, Z. R. Yang, J. H. Zhou, J. Sun, Z. Q. Mao, and M. L. Tian, *Phys. Rev. B* **100**, 205124 (2019).
- [38] Preliminary DFT calculations on the pressure dependency of the Raman phonon mode frequencies and linewidths hint at possible anharmonicity effect with increasing pressure. Details will be presented in a subsequent paper.
- [39] A. Bera, K. Pal, D. V. S. Muthu, S. Sen, P. GuptaSarma, U. V. Waghmare, and A. K. Sood, *Phys. Rev. Lett.* **110**, 107401 (2013).
- [40] F. D. Murnaghan, *Proc. Natl. Acad. Sci. USA* **30**, 244 (1944).
- [41] M. Hanfland, H. Beister, and K. Syassen, *Phys. Rev. B* **39**, 12598 (1989).
- [42] A. Topp, J. M. Lippmann, A. Varykhalov, V. Duppel, B. V. Lotsch, C. R. Ast, and L. M. Schoop, *New J. Phys.* **18**, 125014 (2016).
- [43] M. M. Hosen, K. Dimitri, I. Belopolski, P. Maldonado, R. Sankar, N. Dhakal, G. Dhakal, T. Cole, P. M. Oppeneer, D. Kaczorowski, F. Chou, M. Z. Hasan, T. Durakiewicz, and M. Neupane, *Phys. Rev. B* **95**, 161101(R) (2017).
- [44] Y. Zhang, C. Wang, L. Yu, G. Liu, A. Liang, J. Huang, S. Nie, X. Sun, Y. Zhang, B. Shen, H. Liu, U. Weng, L. Zhao, G. Chen, X. Jia, C. Hu, Y. Ding, W. Zhao, Q. Gao, C. Li, S. He, L. Zhao, F. Zhang, S. Zhang, F. Yang, Z. Wang, Q. Peng, X. Dai, Z. Fang, Z. Xu, C. Chen, and X. J. Zhou, *Nat. Commun.* **8**, 15512 (2017).
- [45] B. Xu, L. X. Zhao, P. Marsik, E. Sheveleva, F. Lyzawa, Y. M. Dai, G. F. Chen, X. G. Qiu, and C. Bernhard, *Phys. Rev. Lett.* **121**, 187401 (2018).
- [46] J. Hu, Z. Tang, J. Liu, X. Liu, Y. Zhu, D. Graf, K. Myhro, S. Tran, C. N. Lau, J. Wei, and Z. Mao, *Phys. Rev. Lett.* **117**, 016602 (2016).
- [47] J. Hu, Y. L. Zhu, D. Graf, Z. J. Tang, J. Y. Liu, and Z. Q. Mao, *Phys. Rev. B* **95**, 205134 (2017).
- [48] J. Hu, Z. Tang, J. Liu, Y. Zhu, J. Wei, and Z. Mao, *Phys. Rev. B* **96**, 045127 (2017).
- [49] M. Hangyo, S.-I. Nakashima, and A. Mitsuishi, *Ferroelectrics* **52**, 151 (1983).
- [50] A. S. Pine and G. Dresselhaus, *Phys. Rev. B* **5**, 4087 (1972).
- [51] C.-H. Lee, E. Cruz-Silva, L. Calderin, M. J. Hallander, B. Bersch, T. E. Mallouk, and J. A. Robinson, *Sci. Rep.* **5**, 10013 (2015).
- [52] J. Khan, C. M. Nolen, D. Teweldebrhan, D. Wickramaratne, R. K. Lake, and A. A. Balandin, *Appl. Phys. Lett.* **100**, 043109 (2012).
- [53] M. Zhang, X. Wang, A. Rahman, Q. Zeng, D. Huang, R. Dai, Z. Wang, and Z. Zhang, *Appl. Phys. Lett.* **112**, 041907 (2018).

- [54] K. Syassen, *High Press. Res.* **28**, 75 (2008).
- [55] H. K. Mao, J. Xu, and P. M. Bell, *J. Geophys. Res.* **91**, 4673 (1986).
- [56] A. Sharafeev, V. Gnezdilov, R. Sankar, F. C. Chou, and P. Lemmens, *Phys. Rev. B* **95**, 235148 (2017).
- [57] R. Boehler, *Rev. Sci. Instrum.* **77**, 115103 (2006).
- [58] R. Boehler and K. De Hantsetters, *High Press. Res.* **24**, 391 (2004).
- [59] G. J. Piermarini, S. Block, and J. D. Barnett, *J. Appl. Phys.* **44**, 5377 (1973).
- [60] G. J. Piermarini, S. Block, J. D. Barnett, and R. A. Forman, *J. Appl. Phys.* **46**, 2774 (1975).
- [61] O. D. Rigaku, CrysAlisPro 1.171.38.46, Rigaku Oxford Diffraction, 2017.
- [62] P. Blaha, K. Schwarz, G. K. H. Madsen, D. Kvasnicka, J. Luitz, F. Tran, and L. D. Marks, *Wien2k, an Augmented Plane Wave + Local Orbitals Program for Calculating Crystal Properties* (Karlheinz Schwarz, Techn. Universität Wien, Austria, 2018).
- [63] Anton Kokalj, *J. Mol. Graphics Modell.* **17**, 176 (1999).
- [64] G. Kresse and J. Furthmüller, *Comput. Mater. Sci.* **6**, 15 (1996).
- [65] G. Kresse and J. Furthmüller, *Phys. Rev. B* **54**, 11169 (1996).
- [66] G. Kresse and J. Hafner, *Phys. Rev. B* **49**, 14251 (1994).
- [67] G. Kresse and J. Hafner, *Phys. Rev. B* **47**, 558 (1993).
- [68] J. P. Perdew, K. Burke, and M. Ernzerhof, *Phys. Rev. Lett.* **77**, 3865 (1996).
- [69] J. P. Perdew, K. Burke, and M. Ernzerhof, *Phys. Rev. Lett.* **78**, 1396 (1997).
- [70] S. Grimme, J. Antony, S. Ehrlich, and H. Krieg, *J. Chem. Phys.* **132**, 154104 (2010).
- [71] B. Salmankurt and S. Duman, *Philos. Mag.* **97**, 175 (2017).
- [72] H. Yuan, X. Zhou, Y. Cao, Z. Zhang, H. Sun, S. Li, Z. Shao, J. Hu, Y. Zhu, Z. Mao, and M. Pan, *npj 2D Mater. Appl.* **3**, 12 (2019).